Version of Record: https://www.sciencedirect.com/science/article/pii/S0168945219315250
Manuscript_0f4121754709e2ab01a3bdcf47632264

Protein synthesis increases with photosynthesis via the stimulation of translation initiation

Guillaume Tcherkez[1,2*], Adam Carroll[3], Cyril Abadie[2], Samuel Mainguet[4], Marlène Davanture[5] and Michel Zivy[5]

1. Research School of Biology, ANU Joint College of Sciences, Australian National University, 2601 Canberra ACT, Australia.
2. Institut de Recherche en Horticulture et Semences, INRA, Université d'Angers, 42 rue Georges Morel, 49070 Beaucouzé, France.
3. Joint Mass Spectrometry Facility, Research School of Chemistry, Australian National University, 2601 Canberra ACT, Australia.
4. Institute of Plant Sciences of Saclay, INRA, University Paris-Sud, CNRS, Université Paris-Saclay, Ferme du Moulon, 91190 Gif-sur-Yvette, France.
5. Plateforme d'Analyse de Protéomique Paris Sud-Ouest (PAPPSO), GQE Le Moulon, INRA, Univ. Paris-Sud, CNRS, AgroParisTech, Université Paris-Saclay, Ferme du Moulon, 91190 Gif-sur-Yvette, France.

*Contact author to whom correspondence should be addressed: Tel. +61 (0)2 6125 0381. E-mail. guillaume.tcherkez@anu.edu.au

Keywords: photosynthesis, photorespiration, protein synthesis, translation, phosphorylation

Number of figures: 4

Number of tables: 1

Word count (w/o abstract, acknowledgements and references): 5,205

Twitter accounts: @ANUmedia; @IRHS_Seed_lab

ORCID numbers:
Guillaume Tcherkez: 0000-0002-3339-956X

Abstract (198 words)

Leaf protein synthesis is an essential process at the heart of plant nitrogen (N) homeostasis and turnover that preferentially takes place in the light, that is, when N and CO_2 fixation occur. The carbon allocation to protein synthesis in illuminated leaves generally accounts for *ca*. 1% of net photosynthesis. It is likely that protein synthesis activity varies with photosynthetic conditions (CO_2/O_2 atmosphere composition) since changes in photorespiration and carbon provision should in principle impact on amino acid supply as well as metabolic regulation via leaf sugar content. However, possible changes in protein synthesis and translation activity when gaseous conditions vary are virtually unknown. Here, we address this question using metabolomics, isotopic techniques, phosphoproteomics and polysome quantitation, under different photosynthetic conditions that were varied with atmospheric CO_2 and O_2 mole fraction, using illuminated Arabidopsis rosettes under controlled gas exchange conditions. We show that carbon allocation to proteins is within 1–2.5% of net photosynthesis, increases with photosynthesis rate and is unrelated to total amino acid content. In addition, photosynthesis correlates to polysome abundance and phosphorylation of ribosomal proteins and translation initiation factors. Our results demonstrate that translation activity follows photosynthetic activity, showing the considerable impact of metabolism (carboxylation–oxygenation balance) on protein synthesis.

1. Introduction

It is now nearly 250 years since proteins were extracted and purified from green leaves for the first time [1] and nearly 85 years since protein synthesis (and degradation) activity by leaves was first shown [2-4]. Yet, physiological mechanisms that dictate leaf protein content are presently incompletely understood, and this represents a hurdle in the understanding of leaf primary carbon and nitrogen (N) metabolism. In fact, a considerable proportion of leaf proteins is made of ribulose 1,5-bisphosphate carboxylase/oxygenase (Rubisco) and carbonic anhydrase and is thus directly involved in photosynthetic CO_2 assimilation. The turnover of leaf proteins is the cornerstone of N metabolism, since proteins such as Rubisco are remobilized and used as a N (and sulphur) reservoir during grain filling, fruit development and leaf senescence. Also, protein degradation is regulated by N availability, environmental and internal signals, allowing optimal plant N partitioning and growth [5]. However, relatively little is known about the fast control of protein synthesis in response to common situations in leaves (such as varying CO_2), in contrast with seedlings and roots in which the control of translation under hypoxia has been well-studied. In other words, the regulation of leaf protein synthesis and turnover in the short-term is much less understood.

It has been shown that there is a diurnal cycle of protein synthesis activity, with higher translation activity (and higher polysome abundance) in the light compared with the dark [6-9]. Also, protein synthesis has been suggested to relate to growth rate [10] and sucrose content in the dark [7]. In addition, the effect of light as compared to the dark has been shown to correlate with the phosphorylation of translation initiation factors (eIFs) and ribosomal proteins (such as RPS6), indicating that the control of cytosolic translation initiation plays an important role in circadian (dark/light) protein synthesis regulation [11-14]. Accordingly, pioneering works using isotopic labelling (with ^{15}N) demonstrated that leaf protein synthesis took place in the light (from nitrate) and was negligible in darkness [15].

In principle, the photosynthetic rate itself (and therefore, atmospheric gaseous composition) can be anticipated to have an effect on protein synthesis and translation activity. In particular, translation initiation involves several molecular actors that can be associated with metabolic regulation. Briefly, translation initiation starts with the formation of a 43S preinitiation complex, which contains the 40S ribosome subunit and eIFs 5, 3, 1 and 1A. The preinitiation complex binds the eIF2 complex and then the mRNA-eIF(iso)4F complex (here, parentheses mean two complexes, eIF4F and eIFiso4F). The plant-specific eIFiso4F complex comprises eIFs 4A, 4B, iso4G, iso4E and poly-A binding proteins. After mRNA scanning and start codon identification, some eIFs are liberated, the ribosomal 60S subunit binds and elongation starts [12, 16].

Many eIFs or ribosomal proteins (RPs) can be modified post-translationally (in particular, by phosphorylation) and this modulates their activity [17]. In yeast, General Control Non-derepressible 2 (GCN2) can phosphorylate eIF2α under specific nutrient or redox conditions [see, e.g., [18]], preventing guanyl nucleotide recycling. Also, metabolic conditions (sugar and free amino acid content) can impact on the mammalian target of rapamycin (mTOR) signaling pathway which controls RPS6 phosphorylation (for a recent experimental study in Arabidopsis, see [19]) as well as the sugar-sensing kinase SnRK1 which can phosphorylate eIF(iso)4E [20]. Therefore, it has been hypothesized that photosynthetic activity promotes phosphorylation of RPS6 (amongst other RPs) and the initiation factor eIF4B, and disfavor phosphorylation of eIF2α, thus stimulating protein synthesis [11]. Furthermore, CO_2 and O_2 mole fractions dictate the rate of photorespiration, which could also impact on translation. On the one hand, photorespiration leads to peroxisomal H_2O_2 generation and can induce oxidative stress and perhaps, this might trigger phosphorylation of eIF2α [21] thereby inhibiting

translation initiation. However, on the other hand, photorespiration produces amino acids (glycine, serine), leads to mitochondrial ATP generation and enhance N assimilation, and this might be accompanied by an increased protein synthesis. Nevertheless, it should be noted that the specific role of GCN proteins is still unclear, and other kinases (such as casein kinase 2, CK2) are capable of phosphorylating eIF2α *in vitro* [12, 22-25]. Also, an important role of SnRK1 (also involved in sucrose signaling) has been recently shown for eIF4(iso)4G phosphorylation in response to submergence [26].

Up to now, there is limited information on the rate of protein synthesis when photosynthesis varies, typically when CO_2 and/or O_2 mole fraction changes. The use of ^{15}N labelling in barley leaves has suggested that protein synthesis correlated with chlorophyll content and thus potentially with photosynthesis [27]. Also, ^{15}N labelling in proteins has been found to be much larger with CO_2 in air compared to CO_2-free air, suggesting a coupling with photosynthesis [15]. In photosynthetizing leaves, isotopic pulse labelling (with $^{14}CO_2$) has demonstrated that protein synthesis represents a carbon flux of about 0.1 µmol m^{-2} s^{-1} and after sugar export has taken place (i.e. after several hours in darkness), ^{14}C-labelled proteins can represent up to 20% of total leaf radioactivity [28-31] – such a proportion being changed by the presence of close sink organs [32] and leaf age [28]. When photosynthesis with $^{14}CO_2$ was augmented via incident light intensity, proteins represented a lower percentage of total leaf radioactivity but in absolute terms, represented more labelled carbon, with a ^{14}C-flux of ≈0.1 µmol m^{-2} s^{-1} at low light and ≈0.25 µmol m^{-2} s^{-1} at high light [33]. In a previous study, we observed that the phosphorylation of some eIFs and RPs could respond to CO_2 mole fraction, suggesting there is a an increase of translation activity when photosynthesis increases [11].

However, there is presently no specific study exploring and quantifying the impact of photosynthetic conditions on leaf protein synthesis and in particular, the short-term effect of CO_2 and O_2 mole fraction (and thus the balance between gross photosynthesis and photorespiration). This lack of knowledge is problematic because the turnover rate of proteins may affect not only N assimilation but also photosynthetic capacity itself. In fact, while it is rather unlikely that the very high Rubisco content changes dramatically in the short-term when photosynthesis varies, the pool of less abundant proteins involved in the Calvin cycle (including Rubisco activase or enzymes with a high control coefficient in the cycle) or light reactions could change within a few hours. In fact, ^{15}N labelling has recently shown that some proteins involved in photosynthesis have a short half-life, such as Rubisco activase (turnover rate ≈0.2 d^{-1}) [34].

Here, we took advantage of omics analyses performed on Arabidopsis rosettes, using gas-exchange under controlled conditions (CO_2, O_2, light/dark) and sampling by instant liquid nitrogen spraying using our system previously described in [35]. Here, it was further combined to isotopic techniques and polysome quantitation to elucidate the potential effect of short-term changes in CO_2 and O_2 mole fraction on protein synthesis. The use of $^{13}CO_2$ labelling allowed us to quantify the amount of carbon allocated to protein synthesis, while polysome relative quantitation as well as eIFs and RPs phosphorylation analysis (in particular RPS6 phosphorylation) gave information on translation activity. The objective of the present study is not to dissect molecular mechanism of translational control but rather, to look at potential changes in protein synthesis with photosynthesis. In fact, our results demonstrate that protein synthesis follows the photosynthesis rate and is unrelated to total amino acid availability, suggesting a control of translation initiation by metabolic signaling driven by the carboxylation-oxygenation balance.

2. Material and methods

2.1. Plant material

After sowing on potting mix, *Arabidopsis thaliana* (Col-0 accession) plantlets were transplanted to individual pots and grown for 6 weeks in a controlled environment (growth chamber) under short days. Conditions were as follows: 8:16 h light/dark at an irradiance of approximately 100 µmol photons m^{-2} s^{-1}, 20/18°C day/night temperature, 65% humidity and nutrient solution (1 g L^{-1} PP14-12-32, [Plant-Prod, Puteaux, France] supplemented with 20 µL L^{-1} fertoligo L [Fertil, Boulogne-Billancourt, France]) twice a week.

2.2. Metabolomics

Metabolomics profiling was performed as in [36]. Briefly, 20 mg of leaf powder from lyophilized leaf samples were extracted with 2 mL methanol:water (70:30 v/v). The supernatant was vacuum dried and chemically derivatized with methoxyamine and MSTFA in pyridine. Ribitol was added as an internal standard, as well as an alkane mix to calibrate retention index. GC-MS metabolomics analyses were carried out using a Pegasus III GC-TOF-MS system (Leco, France). Peak integration was verified manually for all metabolites to avoid erroneous determinations by the Pegasus software.

2.3. Gas exchange and sampling

Arabidopsis plants were taken at fixed time of day in the controlled growth chamber (after about 4 h light) and used for gas-exchange and labelling. Gas exchange and sampling were carried out as in [37]. Briefly, photosynthesis and respiration rates were monitored with the gas exchange open system LI-COR 6400/XT (LI-COR, Austin, USA), under a controlled humidity of 80% fixed with a dew-point generator (LI-COR 610). Net photosynthesis (*A*) was measured in typical conditions (desired CO_2 mole fraction, 21% O_2, 22°C, 280 µmol m^{-2} s^{-1} PAR [photosynthetically active radiation], 10% blue). CO_2 mole fraction was either 100, 380 or 1000 µmol mol^{-1}. O_2 mole fraction was either 0% (pure N_2 used as inlet gas), 21% (ordinary air) or 100% (pure O_2). CO_2-free conditions (no CO_2 in inlet gas) were not used here since no ^{13}C labelling would have been possible. Gas-exchange was carried out with a purpose-built chamber adapted to three *Arabidopsis* rosettes connected to the sample channel of the LI-COR 6400 *xt*. Air temperature in the chamber was maintained with a water-bath. Leaf rosettes were separated from the below-ground part and soil of the pot by a Plexiglas wall (with specific holes for collars sealed with Terostat®) so as to avoid alteration of gas-exchange by soil and root respiration. The upper wall of the leaf chamber was made of a tight polyvinyl chloride film allowing very fast quenching by liquid N_2 freezing. Further details on the chamber can be found in our previous studies [11, 35, 37]. Photosynthesis was allowed to stabilise under the desired CO_2 and O_2 mole fraction (at 280 µmol photon m^{-2} s^{-1} PAR) and after 3 hours, rosettes were instantly frozen and stored at –80°C for further analyses. Rosettes sampled in darkness were collected after 3 hours at 380 µmol mol^{-1} CO_2 and 21% O_2 in the light and then 2 hours of dark-adaptation. Isotopic labelling was carried out with $^{13}CO_2$ (99% ^{13}C, Sigma Aldrich) for 4 hours in the O_2/CO_2 conditions of interest, and sampling was carried out as above at the end of the 4-h labelling time by liquid N_2 freezing.

2.4. Phosphoproteomics

The protocol used to carry out quantitative phosphoproteomics analyses was similar to that previously described in [35]. Total (non-phosphorylated) protein analysis was also performed on the same samples to quantify total protein abundance (and therefore check that changes in phosphorylation level are not simply due to changes in total protein content). Protein extraction was carried out using the trichloroacetate/acetone method and protein digestion was performed at an enzyme-to-substrate ratio of 1:50 (w:w) overnight at 37°C with sequencing-grade trypsin (Promega). Stable isotope dimethyl labelling was done according to the on-column protocol of [38] using three different isotopologues of formaldehyde (CH_2O, C^2H_2O and $^{13}C^2H_2O$) thereby allowing simultaneous injection of three extracts (each triplet is referred to as 'triplex'). A sample made of the mixture of all of the samples was dimethylated (with unlabeled methyl groups) and used as a reference in all triplexes. The use of triplexes thus allowed us to analyze two samples per injection (intermediate and heavy labeling). After being spin-dried and resuspended in acetonitrile/formic acid solution, peptides were subjected to SCX (Strong Cation Exchange) chromatography. Collected fractions were enriched in phosphopeptides by IMAC (Immobilized ion Metal Affinity Chromatography) [39] and then analysed by nanoLC-MS/MS using a NanoLC-Ultra system (Eksigent). Peptides eluted from a 35-min long, 5-to-35% acetonitrile gradient were analysed with a coupled Q-Exactive mass spectrometer (Thermo Electron). A "Top 8" cycle of data-dependent acquisition was used (i.e., the 8 major ions detected in each MS spectrum were submitted to MS/MS fragmentation). Resolution for precursors and fragments was set to 70,000 and 17,500 respectively. Collision energy was set at 27% and exclusion time at 40 s.

For identification of peptides, phosphorylation sites and quantification, database searches were performed using X!Tandem Sledgehammer (2013.09.01.1) [40] with the TAIR database (www.arabidopsis.org). Cysteine carboxyamidomethylation and light, intermediate and heavy dimethylation of peptide N-termini and lysine residues were set as static modifications while methionine oxidation and phosphorylation of tyrosine, serine or threonine residues were set as variable modifications. Mass error tolerance was 10 ppm for precursors and -0.02 Th for fragments. Identified proteins were filtered and grouped using the X!Tandem pipeline v3.3.1 (http://pappso.inra.fr/bioinfo/xtandempipeline/) [41]. Relative quantification of non-phosphorylated peptides and phosphopeptides was performed using the MassChroQ software [42] by extracting ion chromatograms (XICs) of all identified peptides within a 5 ppm window and by integrating the area of the XIC peak at their corresponding retention time, after LC-MS/MS chromatogram alignment.

2.5. Isotopic measurements in proteins

Proteins were purified from frozen samples (50 mg fresh weight). First, a raw proteic extract was obtained using a trichloroacetate-acetone extraction as above. Then proteins were purified after [43] with the following modifications: the dry pellet (proteins and cell wall debris obtained in the trichloroacetate-acetone extraction) was dissolved in 1.5 mL resuspension buffer (1% SDS, 150 mM Tris-HCl, 0.1 mM dithiotreitol, 1 mM EDTA). After centrifugation at 10,000 g for 5 min at 14°C, the supernatant was collected and proteins were precipitated by adding 1.5 mL methanol. After centrifugation (10,000 g, 5 min, 14°C), the supernatant was discarded and the protein pellet rinsed with 1.5 mL methanol and centrifuged. The pellet was then freeze-

dried, weighed in tin capsules and analysed. Isotopic analysis was done using an elemental analyser (Carlo-Erba) coupled to an isotope ratio mass spectrometer (Isoprime, Elementar) run in continuous flow. All sample batches included standards (sucrose, glycine, cysteine; previously calibrated against IAEA standards glutamic acid USGS-40 and caffeine IAEA-600) each twelve samples. The isotope composition ($\delta^{13}C$) was then converted to $\%^{13}C$.

2.6. Polysome abundance

Polysome abundance was determined by sucrose density gradient centrifugation analysis from liquid-nitrogen frozen rosettes (protocol explained in Supplemental Methods).

2.7. Statistics

Phosphoproteomics and metabolomics analyses were carried out 3 to 6 times for each condition. Peptides considered to vary significantly between photosynthetic (CO_2/O_2 and/or light/dark) conditions were those with $P<0.05$ using ANOVA (Fig. 4). This value ensured an acceptable false discovery rate (FDR), estimated as in Tan & Xu (2014), including the Hochberg-Benjamini correction (Hochberg & Benjamini 1990), over the whole dataset. A multivariate analysis was carried out with orthogonal projection on latent structures (OPLS, with phosphopeptides or metabolites as X variables and O_2/CO_2 conditions as a quantitative Y variable) carried out with Simca (MKS Umetrics, Sweden) [44, 45]. The effect of each phosphopeptide or metabolite in explaining the X-Y relationship was quantified using the loading along axis 1 ($p_{corr}(1)$) and the *P*-value of the ANOVA in a volcano plot. The robustness of the OPLS model was assessed with the correlation coefficient between prediction and observations (R^2), the cross-validated correlation coefficient (Q^2) and the intercept of the response of Q^2 to similarity in iterated (250 iterations) permutations tests (Q^2_{int}). The statistical significance of the OPLS model was tested using a χ^2 test on the comparison with a random model (mean ± random error). The associated *P*-value was denoted as $P_{CV\text{-}ANOVA}$.

3. Results

3.1. Photosynthesis and metabolism

Six gas-exchange conditions were used, with CO_2 mole fraction of 100, 380 or 1000 µmol mol^{-1} under 21% O_2, and O_2 mole fraction of 0% (pure N_2 used as background gas), 21% or 100% (pure O_2 as background gas) at 380 µmol mol^{-1} CO_2. Analyses were also conducted in dark-adapted rosettes after photosynthesis under standard (21% O_2, 380 µmol mol^{-1} CO_2) conditions. Changes in photosynthetic conditions were associated with considerable changes in metabolite content. Metabolomics analyses by GC-MS showed that amongst the 108 analytes detected, 31 were associated with significant changes ($P<0.01$ with an ANOVA) with O_2/CO_2 conditions (Fig. 1a). They could be grouped into three clusters. The first cluster comprised alanine and tyrosine, considerably increased with N_2 (0% O_2) as inlet air (meaning ≈0.02% O_2 in air surrounding leaves due to photosynthetic O_2 evolution). The second cluster comprised metabolites particularly accumulated at very high photorespiration (low photosynthesis), such as glycine and serine (photorespiration intermediates) but also other amino acids such as cysteine, threonine and valine, or organic acids such as succinate. The third cluster comprised metabolites present under normoxic conditions and decreased under 0% O_2 inlet air, such as glycolate (photorespiration intermediate), fumarate or putrescine. Unsurprisingly, several metabolites (including sugars and photorespiratory intermediates glycine and serine) were affected by darkness as compared to the light (Fig. S2). Multivariate analysis yielded a very good OPLS model ($R^2 = 0.965$; $Q^2 = 0.934$) that was robust (negative Q^2_{int} at –0.501) and highly significant ($P_{CV\text{-}ANOVA} = 4 \cdot 10^{-14}$) (Fig. S1). The volcano plot that combines univariate and multivariate analysis showed that best biomarkers of O_2/CO_2 conditions were succinate, serine, glycine, pipecolate and cysteine (decreased with photosynthesis), and alanine and homoserine (increased at high photosynthesis) (Fig. 1b).

As expected, there was a clear increase in the photosynthesis rate as O_2/CO_2 decreased (showing the inhibition of photorespiration and augmented carboxylation as the O_2-to-CO_2 ratio decreased), with a significant depressing effect of low O_2 (Fig. 1c). There was no significant effect of O_2 mole fraction on the rate of dark respiration (CO_2 evolution in darkness). The sum of proteogenic amino acids (expressed in signal % of total recovered metabolites) tended to increase as CO_2 increased from 100 to 1000 µmol mol^{-1}, but there was also a high content in amino acids at very high photorespiration (100% O_2) and in darkness (Fig. 1d). These effects were driven by the accumulation of alanine at low O_2, the build-up of glycine and serine at 100% O_2, and the proportional lower content in sugars in darkness. The impact of photorespiration on glycine and serine metabolism was also visible with the glycine-to-serine ratio that increased considerably under 100% O_2 (Fig. 1e).

3.2. Carbon allocation to protein synthesis

Isotopic labelling with $^{13}CO_2$ during photosynthesis was carried out in order to follow the metabolic partitioning of fixed carbon into proteins. Labelling with $^{13}CO_2$ was obviously not performed in the dark since there was no photosynthetic CO_2 fixation. There was a clear ^{13}C incorporation into proteins as shown by the ^{13}C percentage above natural abundance (Fig. 2a). When converted into absolute units (accounting for both leaf protein content and % ^{13}C), the allocation flux to proteins increased up to four times as the O_2/CO_2 ratio decreased showing the

impact of source carbon fixation to protein synthesis (Fig. 2b). In fact, at low oxygen, the ^{13}C flux represented about 0.2 µmol m^{-2} s^{-1}. However, when normalized to photosynthesis, allocation fell within a narrow range of 1 to 2.5% of photosynthesis, with higher values at 100% O_2 perhaps suggesting a specific effect of high oxygen on protein synthesis.

3.3. Polysome abundance

Polysome abundance was measured using the gradient method based on absorbance at 260 nm using the signal of the polysome gradient region (Fig. 3a). There was a substantial difference in particular when comparing low O_2/CO_2 to other conditions: in fact, when expressed in normalized units (% of total trace signal), polysome relative abundance was significantly higher at high photosynthesis (Fig. 3b). Polysome abundance tended to be lower at high photorespiration (100% O_2) compared to that in darkness. Also, as expected, there was a significant effect of O_2 mole fraction in darkness with less polysomes at low oxygen, highlighting the specific effect of hypoxia. Of course, this analysis encompasses all polysome fractions in the same peak (organellar and cytosolic) but taken as a whole, the polysome content was found to be affected by gaseous conditions, and in the light, correlated to the photosynthetic rate.

3.4. Phosphorylation of eIFs and RPs

The phosphoproteomics analysis allowed the detection and quantification of 2,057 phosphopeptides (representing 1,044 individual proteins), among which 69 (3.3%) were associated with protein synthesis (translation elongation factors, translation initiation factors, ribosomal proteins and other proteins associated with translation). The list of unique phosphopeptides is provided in Table 1 and some of them are illustrated in Fig. 4. Phosphosites identified here have been found previously, except for two of them: Ser 47/Thr 51 in the nucleus-encoded chloroplastic ribosomal protein RPS9 (AT1G74970), and Ser 149 of eIF2Bδ (AT1G48970) (Table 1). Phosphopeptides were filtered to carry out statistics, by keeping only those with less than 20% missing values. Univariate analysis with ANOVA conducted with the 69 translation-related phosphopeptides, showed that 17 phosphopeptides were significantly affected by O_2/CO_2 conditions, representing 11 proteins (Fig. 4a). Hierarchical clustering showed that there were distributed in two groups. The first cluster was assocatied with higher phosphorylation at high photosynthesis and comprised RPS6A and RPS6B at phosphosite Ser 240 (detailed in Fig. 4b). The second cluster was associated with lower phosphorylation as photosynthesis increased (and higher phosphorylation in the dark) and comprised eIF4G at phosphosites Ser 178 (detailed in Fig. 4b). Multivariate analysis conducted on the 69 translation-related phosphopeptides yielded a very good OPLS model ($R^2 = 0.954$; $Q^2 = 0.916$) that was robust (negative Q^2_{int} at –0.265) and highly significant ($P_{CV\text{-}ANOVA} = 7 \cdot 10^{-13}$) (Fig. 4c). The volcano plot that combines univariate and multivariate analysis showed that best biomarkers of O_2/CO_2 conditions were RPS6 and eIF3d phosphopeptides (increased with photosynthesis), and eIF4G and eIF5A2 phosphopeptides (decreased at high photosynthesis) (Fig. 4d). Taken as a whole, the phosphopattern found here indicates that phosphorylation that promoted translation (such as RPS6 phosphorylation) increased while phosphorylation that inhibits translation (such as eIF4G) decreased with photosynthesis. Changes observed here in phosphopeptide abundance were not due to changes in total protein amounts but were

effectively due to modifications in phosphorylation level, since none of the significant phosphopeptides were associated with significant variation in total protein content (Fig. S3).

4. Discussion

4.1. Protein synthesis increases with CO_2/O_2

We find that the ^{13}C-flux to proteins increases with photosynthesis (Fig. 2b) and our estimate of the absolute carbon allocation to protein synthesis was 0.1-0.2 µmol m^{-2} s^{-1}, that is, 3 to 6 µg protein m^{-2} s^{-1}. This estimate agrees with the order of magnitude of protein turnover rate estimated using inhibitors (≈0.2 µmol C m^{-2} s^{-1}) [46] or ^{14}C-tracing (between 0.1 and 0.25 µmol m^{-2} s^{-1} depending on light conditions) [33] and the average protein synthesis rate of 6.25 µg protein m^{-2} s^{-1} (assuming a specific leaf area of 180 g FW m^{-2}) found in Arabidopsis rosettes using ^{13}C labelling [6].

The physiological impact of protein synthesis not only relates to carbon allocation but also to energy consumption since translation consumes a substantial amount of ATP. In effect, the average amount of ATP required per amino acid added during translation is about 5 [47]. The order of magnitude of the rate associated with protein synthesis (0.1-0.2 µmol C m^{-2} s^{-1}) represents an ATP budget of ≈0.25 µmol ATP m^{-2} s^{-1}. Of course, the rate of protein synthesis was obtained via isotope labelling and includes not only cytoplasmic but also chloroplastic protein synthesis. Therefore, the ATP demand must be met by both photosynthetic light reactions in the chloroplast and day respiration in the cytoplasm.

It is worth noting that day respiration generates about 0.5 µmol CO_2 m^{-2} s^{-1} [48] i.e. 2.6 µmol ATP m^{-2} s^{-1} (using a conversion factor of 31.5 ATP per catabolized glucose molecule) and thus, protein synthesis represents about 0.25/2.6 = 10% of metabolic energy generated by day respiration. That said, cytoplasmic ATP not only comes from catabolism (reoxidation of NADH produced by day respiratory metabolism) but also from photorespiration (reoxidation of photorespiratory NADH coming from glycine-to-serine conversion), which in turn depends on CO_2 and O_2. The contribution of photorespiration to meet the ATP demand might explain why protein synthesis was found here to decline more slowly than photosynthesis when the O_2/CO_2 ratio increased (i.e., 2% of photosynthesis at high O_2 vs. 1% of photosynthesis at high CO_2; Fig. 2c) despite the down-regulation of translation (further explained below). This would be consistent with the non-quantitative recycling of photorespiratory intermediates such as glycerate at high photorespiration [49]. In other words, ATP that is not used to reform 3-phosphoglycerate from glycerate could have been used by other processes such as protein synthesis.

The increase in ^{13}C-allocation when CO_2/O_2 increased was accompanied by an increased proportion of ribosomes in polysomes (Fig. 3) demonstrating an augmented translational activity. Furthermore, this correlated with a significant increase in RPS6 phosphorylation at Ser 240 (substrate phosphosite of RPS6 kinase) (Fig. 4) which is usually typical of the stimulation of ribosomal activity to initiate translation (but see [50] in yeast). There was also a stimulation of translation initiation via the phosphorylation of a number of eIFs, such as eIF4B2 (further discussed below). Taken as a whole, our data show that when the CO_2-to-O_2 ratio increases, there is an increase in protein synthesis (in absolute terms, i.e. in moles of ^{13}C committed to protein production) and this is reflected by higher translational activity.

4.2. Involvement of protein phosphorylation

In addition to RPS6, we found that other proteins involved in translation were phosphorylated, with significant changes with O_2/CO_2 (Fig. 4). Unfortunately, the role of phosphorylation is not always well-known for many initiation factors eIFs (or ribosomal proteins). Phosphorylation might be linked to mechanisms of regulation of translation under our conditions. For example, it seems that eIF4G phosphorylation (at Ser 178) inhibits translation as photorespiration increases while eIF4B2 and eIF3d phosphorylation stimulates translation as photosynthesis increases (for further details on potential roles of phosphorylation sites, see Supplementary Text). In addition to eIFs, our analysis found that phosphorylation of the elongation factor eEF5A2 (also known as initiation factor eIF5A) anti-correlated with photosynthesis, suggesting that translation down-regulation also involves an inhibition of elongation. While eEF5 phosphorylation (at Ser 2) is poorly documented in plants and has been suggested to have no effect in yeast, eEF5 activity is also known to be controlled by hypusination at the consensus site K-x-G-**(^{Hyp}K)**-H-G-x-A-K in yeast and Mammals (for a review, see [51]). A hypusination site is present in Arabidopsis eEF5 (at Lys 51) and hypusination has been shown to occur in planta [52]. Here, hypusination could not be analyzed (in fact, the hypusination site GKHG is cleaved by trypsin). There was no correlation between translation activity (photosynthesis) and the content in hypusine precursors, polyamines (Fig. S4).

Amongst phosphopeptides with more than 20% missing data, one possessed a clear trend with photosynthesis (missing data mostly corresponded to samples collected in the dark) and was associated with nucleolin (NUC-L1; Table 1). There was a clear positive relationship between photosynthesis and nucleolin phosphorylation (Fig. S5). Nucleolin has been shown to be associated with a variety of cellular processes including in plants [53, 54]. Nucleolin phosphorylation has been extensively documented in Mammals, where CK2-mediated phosphorylation triggers nucleolin relocation to the cytoplasm and stimulates its helicase activity so as to facilitate internal ribosomal entry and translation of specific mRNAs [55-57]. In fact, the phosphosite found here at Ser 163 corresponds to a typical CK2 phosphorylation motif (with at least two acidic residues downstream of phosphorylated Ser) (Table 1).

It is worth noting that RPS6A and B were not the sole RPs detected here, since we also found phosphopeptides associated with RPP1A/2A, significantly less abundant at high photosynthesis (high CO_2, low O_2) (Fig. 4). It suggests that unlike RPS6, phosphorylation of these two RPs inhibits translation. This agrees with the recognized role of phosphorylation at the C-terminus (here, Ser 102/120) by CK2 in promoting RPP1/RPP2 dissociation and RPP1 degradation in yeast [58-60].

4.3. Potential mechanisms

Our data suggest that phosphorylation events play an important role in regulating translation activity when O_2/CO_2 varies, as reflected by the progressive RPS6 phosphorylation. RPS6 is phosphorylated by RPS6 kinase (S6K) which is in turn activated (phosphorylated) via the mTOR pathway. Also recently, in Arabidopsis, MRF1 (MA3 domain-containing translation regulatory factor 1) has been shown to interact physically with eIF4A and appears to be phosphorylated via mTOR [61]. eIF2Bδ1 has recently been shown to be a direct phosphorylation target of mTOR in Arabidopsis (eIF2Bδ1 being more phosphorylated in the presence of sucrose) at the same phosphosite as that found here [62]. More generally, several eIFs have been shown to be amongst phosphorylation targets of the mTOR pathway, such as

eIF4G, eIF4B1, eIF2β1 and eIF6A [62]. Since the mTOR pathway mediates nutrient signaling [63], it might suggest that the cellular content in free sugars and/or amino acids drive the response observed here. However, under our conditions, there was no relationship between total amino acid content and protein synthesis (Figs. 1-3). Similarly, there was no correlation between protein synthesis and sucrose content since sucrose (which was rather variable) appeared to be significantly lower under both low and high O_2 (Fig. S4). To gain insight on possible relationships with metabolites, we conducted a correlation analysis between metabolites and phosphosites (Fig. S6). As expected, multivariate analysis showed there was a positive relationship between significant phosphosites (such as RPS6B) and metabolites driven by O_2/CO_2 such as fructose or alanine (and a negative relationship with photorespiratory metabolites glycine and serine) (Fig. S6a). Direct regression analysis also showed a negative relationship between eIF2Bα phosphorylation (significantly enhanced at 100% O_2, Fig. 4) and sugars maltose and trehalose (Fig. S6b). It is thus likely that metabolic signalling participating in phosphorylation changes involved *(i)* a metabolite other than sucrose or amino acids (such as triose phosphates or trehalose 6-phosphate) and/or *(ii)* another pathway interacting with mTOR, such as SnRK1 signaling which is believed to interact with mTOR, and has been shown to inhibit mTOR-mediated RPS6 phosphorylation in plants [64, 65]. The possible involvement of SnRK1 is further discussed in the Supplementary Text.

4.4. Conclusions and perspectives

Taken as a whole, our results show that cytoplasmic protein synthesis increases with photosynthesis via the stimulation of translation initiation. The molecular mechanism of this effect involves protein phosphorylation, in particular of RPs and eIFs. However, other mechanisms not examined here could have contributed, such as changes in mRNA stability or upstream open reading frames (uORF) translation that can mediate metabolic sensing and control ribosome dissociation from specific mRNAs [66, 67]. We recognize that *(i)* the present analysis was focused on protein synthesis while protein degradation might be affected by photosynthetic conditions and *(ii)* the stimulation of cytoplasmic translation is likely to concern specific mRNAs leading to differential protein turnover (for example, proteins involved in photosynthesis might be synthesized more actively when photosynthesis increases). Also, it could be interesting to examine molecular mechanisms further, for example by measuring mTOR activity in different photosynthetic contexts. These aspects will be addressed in a subsequent study.

Acknowledgements

The authors acknowledge the support by public grants overseen by the French National Research Agency (ANR) through a Jeunes Chercheurs project (contract 12-0001-01) and the *Investissement d'Avenir* program through the Labex Saclay Plant Sciences (ANR-10-LABX-0040-SPS) for a post-doctoral grant (to S.M.). G.T and C.A. also thank the Australian Research Council for its support through a *Future Fellowship* grant, under contract FT140100645. The authors thank the facility *Plateforme Métabolisme-Métabolome* for accessing the GC-MS instrument for metabolomics, and Dr. H. Stuart-Williams (Research School of Biology, ANU) for isotopic measurements. The authors thank Dr. K. Hannan (John Curtin School of Medical Research, ANU) for giving access to instruments to carry out polysome profiling.

Contributions

S.M. did gas exchange experiments and sampling for metabolomics and proteomics, M.D. and M.Z. did phosphoproteomics analyses, C.A. did metabolomics analyses, A.C. did isotopic labelling and polysome profiling, G.T. carried out data integration and wrote the paper, all authors discussed results and amended the manuscript.

References

[1] M. Rouelle, Observations sur les parties vertes des plantes, et sur la matière glutineuse ou végéto-animale, Journal de Médecine Chirurgie et Pharmacie (Paris), 40 (1773) 59-67.

[2] A.C. Chibnall, G. Wiltshire, A study with isotopic nitrogen of protein metabolism in detached runner-bean leaves, New Phytologist, 53 (1954) 38-43.

[3] K. Mothes, Die vakuuminfiltration im ernährungsversuch. (Dargestellt an untersuchungen über die assimilation des ammoniaks), Planta, 19 (1933) 117-138.

[4] H.B. Vickery, G.W. Pucher, R. Schoenheimer, D. Rittenberg, The assimilation of ammonia nitrogen by the tobacco plant: a preliminary study with isotopic nitrogen, Journal of Biological Chemistry, 135 (1940) 531-539.

[5] M. Havé, A. Marmagne, F. Chardon, C. Masclaux-Daubresse, Nitrogen remobilization during leaf senescence: lessons from *Arabidopsis* to crops, Journal of Experimental Botany, 68 (2016) 2513-2529.

[6] H. Ishihara, T. Obata, R. Sulpice, A.R. Fernie, M. Stitt, Quantifying protein synthesis and degradation in *Arabidopsis* by dynamic $^{13}CO_2$ labeling and analysis of enrichment in individual amino acids in their free pools and in protein, Plant Physiology, 168 (2015) 74-93.

[7] S.K. Pal, M. Liput, M. Piques, H. Ishihara, T. Obata, M.C. Martins, R. Sulpice, J.T. van Dongen, A.R. Fernie, U.P. Yadav, Diurnal changes of polysome loading track sucrose content in the rosette of wild-type *Arabidopsis* and the starchless *pgm* mutant, Plant Physiology, 162 (2013) 1246-1265.

[8] M. Piques, W.X. Schulze, M. Höhne, B. Usadel, Y. Gibon, J. Rohwer, M. Stitt, Ribosome and transcript copy numbers, polysome occupancy and enzyme dynamics in Arabidopsis, Molecular Systems Biology, 5 (2009) 314-324.

[9] D.D. Seaton, A. Graf, K. Baerenfaller, M. Stitt, A.J. Millar, W. Gruissem, Photoperiodic control of the *Arabidopsis* proteome reveals a translational coincidence mechanism, Molecular Systems Biology, 14 (2018) Article e7962.

[10] H. Ishihara, T.A. Moraes, E.-T. Pyl, W.X. Schulze, T. Obata, A. Scheffel, A.R. Fernie, R. Sulpice, M. Stitt, Growth rate correlates negatively with protein turnover in *Arabidopsis* accessions, The Plant Journal, 91 (2017) 416-429.

[11] E. Boex-Fontvieille, M. Daventure, M. Jossier, M. Zivy, M. Hodges, G. Tcherkez, Photosynthetic control of *Arabidopsis* leaf cytoplasmic translation initiation by protein phosphorylation, PloS one, 8 (2013) Article e70692.

[12] K.S. Browning, J. Bailey-Serres, Mechanism of cytoplasmic mRNA translation, in: The *Arabidopsis* book, American Society of Plant Biologists, 2015, pp. Article e0176.

[13] M.V. Turkina, H.K. Årstrand, A.V. Vener, Differential phosphorylation of ribosomal proteins in *Arabidopsis thaliana* plants during day and night, PloS one, 6 (2011) Article e29307.

[14] R. Enganti, S.K. Cho, J.D. Toperzer, R.A. Urquidi-Camacho, O.S. Cakir, A.P. Ray, P.E. Abraham, R.L. Hettich, A.G. von Arnim, Phosphorylation of ribosomal protein RPS6 integrates light signals and circadian clock signals, Frontiers in Plant Science, 8 (2018) 2210.

[15] T. Andreyeva, E. Plyshevskaya, A study with N-15 of protein formation in the photosynthetic process, Proceedings of the Academy of Sciences of USSR, Biology Series (Izvestiia Akademii Nauk SSSR. Seria Biologicheskaia), 87 (1952) 301-310.

[16] K.S. Browning, Plant translational machinery, in: S. Howel (Ed.) Molecular biology: the plant sciences, Springer New York, 2014, pp. 129-151.

[17] C. Merchante, A.N. Stepanova, J.M. Alonso, Translation regulation in plants: an interesting past, an exciting present and a promising future, The Plant Journal, 90 (2017) 628-653.

[18] S. Lageix, S. Rothenburg, T.E. Dever, A.G. Hinnebusch, Enhanced interaction between pseudokinase and kinase domains in GCN2 stimulates eIF2α phosphorylation in starved cells, PLoS genetics, 10 (2014) Article e1004326.
[19] T. Dobrenel, E. Mancera-Martínez, C. Forzani, M. Azzopardi, M. Davanture, M. Moreau, M. Schepetilnikov, J. Chicher, O. Langella, M. Zivy, C. Robaglia, L.A. Ryabova, J. Hanson, C. Meyer, The *Arabidopsis* TOR kinase specifically regulates the expression of nuclear genes coding for plastidic ribosomal proteins and the phosphorylation of the cytosolic ribosomal protein S6, Frontiers in Plant Science, 7 (2016) Article 1611.
[20] A.N. Bruns, S. Li, G. Mohannath, D.M. Bisaro, Phosphorylation of *Arabidopsis* eIF4E and eIFiso4E by SnRK1 inhibits translation, The FEBS Journal, (2019) In press.
[21] S. Lageix, E. Lanet, M.-N. Pouch-Pélissier, M.-C. Espagnol, C. Robaglia, J.-M. Deragon, T. Pélissier, Arabidopsis eIF2α kinase GCN2 is essential for growth in stress conditions and is activated by wounding, BMC plant biology, 8 (2008) 134-144.
[22] L. Wang, H. Li, C. Zhao, S. Li, L. Kong, W. Wu, W. Kong, Y. Liu, Y. Wei, J.-K. Zhu, H. Zhang, The inhibition of protein translation mediated by AtGCN1 is essential for cold tolerance in *Arabidopsis thaliana*, Plant, Cell & Environment, 40 (2017) 56-68.
[23] Y. Zhang, Y. Wang, K. Kanyuka, M.A.J. Parry, S.J. Powers, N.G. Halford, GCN2-dependent phosphorylation of eukaryotic translation initiation factor-2α in *Arabidopsis*, Journal of Experimental Botany, 59 (2008) 3131-3141.
[24] M.D. Dennis, K.S. Browning, Differential phosphorylation of plant translation initiation factors by *Arabidopsis thaliana* CK2 holoenzymes, Journal of Biological Chemistry, 284 (2009) 20602-20614.
[25] M.D. Dennis, M.D. Person, K.S. Browning, Phosphorylation of plant translation initiation factors by CK2 enhances the in vitro interaction of multifactor complex components, Journal of Biological Chemistry, 284 (2009) 20615-20628.
[26] H.-Y. Cho, M.-Y.J. Lu, M.-C. Shih, The SnRK1-eIFiso4G1 signaling relay regulates the translation of specific mRNAs in *Arabidopsis* under submergence, New Phytologist, 222 (2019) 366-381.
[27] J. Walkley, Protein synthesis in mature and senescent leaves of barley, New Phytologist, 39 (1940) 362-369.
[28] R. Dickson, P. Larson, Incorporation of ^{14}C-photosynthate into major chemical fractions of source and sink leaves of cottonwod, Plant Physiology, 56 (1975) 185-193.
[29] R.E. Dickson, P.R. Larson, ^{14}C fixation, metabolic labeling patterns, and translocation profiles during leaf development in *Populus deltoides*, Planta, 152 (1981) 461-470.
[30] J. Hellebust, R. Bidwell, Protein turnover in wheat and snapdragon leaves: preliminary investigations, Canadian Journal of Botany, 41 (1963) 969-983.
[31] G. Tcherkez, A.M. Limami, Net photosynthetic CO_2 assimilation: more than just CO_2 and O_2 reduction cycles, New Phytologist, (2019) In press.
[32] N.J. Roberts, R.C. Menary, Partitioning and distribution of ^{14}C in *Boronia megastigma* Nees, Journal of Plant Physiology, 137 (1990) 135-139.
[33] A.J. Escobar-Gutiérrez, J.-P. Gaudillère, Carbon partitioning in source leaves of peach, a sorbitol-synthesizing species, is modified by photosynthetic rate, Physiologia Plantarum, 100 (1997) 353-360.
[34] L. Li, C.J. Nelson, J. Trösch, I. Castleden, S. Huang, A.H. Millar, Protein degradation rate in *Arabidopsis thaliana* leaf growth and development, The Plant Cell, 29 (2017) 207-228.
[35] C. Abadie, S. Mainguet, M. Davanture, M. Hodges, M. Zivy, G. Tcherkez, Concerted changes in the phosphoproteome and metabolome under different CO_2/O_2 gaseous conditions in *Arabidopsis* rosettes, Plant and Cell Physiology, 57 (2016) 1544-1556.

562 [36] C. Bathellier, G. Tcherkez, C. Mauve, R. Bligny, E. Gout, J. Ghashghaie, On the resilience
563 of nitrogen assimilation by intact roots under starvation, as revealed by isotopic and
564 metabolomic techniques, Rapid Communications in Mass Spectrometry, 23 (2009) 2847-2856.
565 [37] E. Boex-Fontvieille, M. Davanture, M. Jossier, M. Zivy, M. Hodges, G. Tcherkez,
566 Photosynthetic activity influences cellulose biosynthesis and phosphorylation of proteins
567 involved therein in *Arabidopsis* leaves, Journal of experimental botany, 65 (2014) 4997-5010.
568 [38] P.J. Boersema, R. Raijmakers, S. Lemeer, S. Mohammed, A.J. Heck, Multiplex peptide
569 stable isotope dimethyl labeling for quantitative proteomics, Nature Protocols, 4 (2009) 484-
570 494.
571 [39] X. Yue, A. Schunter, A.B. Hummon, Comparing multistep immobilized metal affinity
572 chromatography and multistep TiO_2 methods for phosphopeptide enrichment, Analytical
573 Chemistry, 87 (2015) 8837-8844.
574 [40] R. Craig, R.C. Beavis, TANDEM: matching proteins with tandem mass spectra,
575 Bioinformatics, 20 (2004) 1466-1467.
576 [41] O. Langella, B. Valot, T. Balliau, M.l. Blein-Nicolas, L. Bonhomme, M. Zivy,
577 X!TandemPipeline: a tool to manage sequence redundancy for protein inference and
578 phosphosite identification, Journal of Proteome Research, 16 (2016) 494-503.
579 [42] B. Valot, O. Langella, E. Nano, M. Zivy, MassChroQ: a versatile tool for mass
580 spectrometry quantification, Proteomics, 11 (2011) 3572-3577.
581 [43] T. Isaacson, C.M. Damasceno, R.S. Saravanan, Y. He, C. Catalá, M. Saladié, J.K. Rose,
582 Sample extraction techniques for enhanced proteomic analysis of plant tissues, Nature
583 Protocols, 1 (2006) 769-774.
584 [44] L. Eriksson, J. Trygg, S. Wold, CV-ANOVA for significance testing of PLS and OPLS®
585 models, Journal of Chemometrics: A Journal of the Chemometrics Society, 22 (2008) 594-600.
586 [45] M. Bylesjö, M. Rantalainen, O. Cloarec, J.K. Nicholson, E. Holmes, J. Trygg, OPLS
587 discriminant analysis: combining the strengths of PLS-DA and SIMCA classification, Journal
588 of Chemometrics: A Journal of the Chemometrics Society, 20 (2006) 341-351.
589 [46] T.J. Bouma, R. De Visser, J.H.J.A. Janssen, M.J. De Kock, P.H. Van Leeuwen, H.
590 Lambers, Respiratory energy requirements and rate of protein turnover in vivo determined by
591 the use of an inhibitor of protein synthesis and a probe to assess its effect, Physiologia
592 Plantarum, 92 (1994) 585-594.
593 [47] F.W.T. Penning De Vries, The cost of maintenance processes in plant cells, Annals of
594 Botany, 39 (1975) 77-92.
595 [48] G. Tcherkez, P. Gauthier, T.N. Buckley, F.A. Busch, M.M. Barbour, D. Bruhn, M.A.
596 Heskel, X.Y. Gong, K.Y. Crous, K. Griffin, Leaf day respiration: low CO_2 flux but high
597 significance for metabolism and carbon balance, New Phytologist, 216 (2017) 986-1001.
598 [49] C. Abadie, C. Bathellier, G. Tcherkez, Carbon allocation to major metabolites in
599 illuminated leaves is not just proportional to photosynthesis when gaseous conditions (CO_2 and
600 O_2) vary, New Phytologist, 218 (2018) 94-106.
601 [50] S. Yerlikaya, M. Meusburger, R. Kumari, A. Huber, D. Anrather, M. Costanzo, C. Boone,
602 G. Ammerer, P.V. Baranov, R. Loewith, TORC1 and TORC2 work together to regulate
603 ribosomal protein S6 phosphorylation in *Saccharomyces cerevisiae*, Molecular Biology of the
604 Cell, 27 (2016) 397-409.
605 [51] T.E. Dever, E. Gutierrez, B.-S. Shin, The hypusine-containing translation factor eIF5A,
606 Critical Reviews in Biochemistry and Molecular Biology, 49 (2014) 413-425.
607 [52] B. Belda-Palazón, C. Almendáriz, E. Martí, J. Carbonell, A. Ferrando, Relevance of the
608 axis spermidine/eIF5A for plant growth and development, Frontiers in Plant Science, 7 (2016)
609 Article 245.
610 [53] F. Pontvianne, I. Matía, J. Douet, S. Tourmente, F.J. Medina, M. Echeverria, J. Sáez-
611 Vásquez, Characterization of AtNUC-L1 reveals a central role of nucleolin in nucleolus

612 organization and silencing of AtNUC-L2 gene in *Arabidopsis*, Molecular Biology of the Cell,
613 18 (2007) 369-379.
614 [54] M. Tajrishi, R. Tuteja, N. Tuteja, Nucleolin: the most abundant multifunctional
615 phosphoprotein of nucleolus, Communicative and Integrative Biology, 4 (2011) 267-275.
616 [55] D.-m. Wu, P. Zhang, R.-y. Liu, Y.-x. Sang, C. Zhou, G.-c. Xu, J.-l. Yang, A.-p. Tong, C.-
617 t. Wang, Phosphorylation and changes in the distribution of nucleolin promote tumor metastasis
618 via the PI3K/Akt pathway in colorectal carcinoma, FEBS letters, 588 (2014) 1921-1929.
619 [56] N. Tuteja, N.W. Huang, D. Skopac, R. Tuteja, S. Hrvatic, J. Zhang, S. Pongor, G. Joseph,
620 C. Faucher, F. Amalric, A. Falaschi, Human DNA helicase IV is nucleolin, an RNA helicase
621 modulated by phosphorylation, Gene, 160 (1995) 143-148.
622 [57] M. Schwab, C. Dreyer, Protein phosphorylation sites regulate the function of the bipartite
623 NLS of nucleolin, European journal of cell biology, 73 (1997) 287-297.
624 [58] M. Tchórzewski, A. Boguszewska, P. Dukowski, N. Grankowski, Oligomerization
625 properties of the acidic ribosomal P-proteins from *Saccharomyces cerevisiae*: effect of P1A
626 protein phosphorylation on the formation of the P1A-P2B hetero-complex, Biochimica et
627 Biophysica Acta (BBA)-Molecular Cell Research, 1499 (2000) 63-73.
628 [59] P. Hasler, N. Brot, H. Weissbach, A.P. Parnassa, K.B. Elkon, Ribosomal proteins P0, P1,
629 and P2 are phosphorylated by casein kinase II at their conserved carboxyl termini, Journal of
630 Biological Chemistry, 266 (1991) 13815-13820.
631 [60] G. Nusspaumer, M. Remacha, J.P.G. Ballesta, Phosphorylation and N-terminal region of
632 yeast ribosomal protein P1 mediate its degradation, which is prevented by protein P2, The
633 EMBO Journal, 19 (2000) 6075-6084.
634 [61] D.-H. Lee, S.J. Park, C.S. Ahn, H.-S. Pai, *MRF* family genes are involved in translation
635 control, especially under energy-deficient conditions, and their expression and functions are
636 modulated by the TOR signaling pathway, The Plant Cell, 29 (2017) 2895-2920.
637 [62] J. Van Leene, C. Han, A. Gadeyne, D. Eeckhout, C. Matthijs, B. Cannoot, N. De Winne,
638 G. Persiau, E. Van De Slijke, B. Van de Cotte, Capturing the phosphorylation and protein
639 interaction landscape of the plant TOR kinase, Nature Plants, 5 (2019) 316-327.
640 [63] Y. Xiong, J. Sheen, The role of target of rapamycin signaling networks in plant growth and
641 metabolism, Plant Physiology, 164 (2014) 499-512.
642 [64] E. Nukarinen, T. Nägele, L. Pedrotti, B. Wurzinger, A. Mair, R. Landgraf, F. Börnke, J.
643 Hanson, M. Teige, E. Baena-Gonzalez, W. Dröge-Laser, W. Weckwerth, Quantitative
644 phosphoproteomics reveals the role of the AMPK plant ortholog SnRK1 as a metabolic master
645 regulator under energy deprivation, Scientific Reports, 6 (2016) Article 31697.
646 [65] E. Baena-González, J. Hanson, Shaping plant development through the SnRK1–TOR
647 metabolic regulators, Current Opinion in Plant Biology, 35 (2017) 152-157.
648 [66] A. Srivastava, Y. Lu, G. Zinta, Z. Lang, J. Zhu, UTR-dependent control of gene expression
649 in plants, Trends in Plant Science, 23 (2018) 248-260.
650 [67] A.G. von Arnim, Q. Jia, J.N. Vaughn, Regulation of plant translation by upstream open
651 reading frames, Plant Science, 214 (2014) 1-12.
652 [68] A. Mustroph, M.E. Zanetti, C.J.H. Jang, H.E. Holtan, P.P. Repetti, D.W. Galbraith, T.
653 Girke, J. Bailey-Serres, Profiling translatomes of discrete cell populations resolves altered
654 cellular priorities during hypoxia in *Arabidopsis*, Proceedings of the National Academy of
655 Sciences, 106 (2009) 18843-18848.
656 [69] B. Bai, A. Peviani, S. van der Horst, M. Gamm, B. Snel, L. Bentsink, J. Hanson, Extensive
657 translational regulation during seed germination revealed by polysomal profiling, New
658 Phytologist, 214 (2017) 233-244.
659 [70] T.C. Vary, C.J. Lynch, Nutrient signaling components controlling protein synthesis in
660 striated muscle, The Journal of Nutrition, 137 (2007) 1835-1843.

[71] J. Ling, S.J. Morley, J.A. Traugh, Inhibition of cap-dependent translation via phosphorylation of eIF4G by protein kinase Pak2, The EMBO Journal, 24 (2005) 4094-4105.
[72] S.J. Morley, P.S. Curtis, V.M. Pain, eIF4G: translation's mystery factor begins to yield its secrets, RNA, 3 (1997) 1085-1104.
[73] A. Marintchev, G. Wagner, Translation initiation: structures, mechanisms and evolution, Quarterly Reviews of Biophysics, 37 (2004) 197-284.
[74] M. Schepetilnikov, M. Dimitrova, E. Mancera-Martínez, A. Geldreich, M. Keller, L.A. Ryabova, TOR and S6K1 promote translation reinitiation of uORF-containing mRNAs via phosphorylation of eIF3h, The EMBO journal, 32 (2013) 1087-1102.
[75] H. Ehsan, W.K. Ray, B. Phinney, X. Wang, S.C. Huber, S.D. Clouse, Interaction of *Arabidopsis* BRASSINOSTEROID-INSENSITIVE 1 receptor kinase with a homolog of mammalian TGF-β receptor interacting protein, The Plant Journal, 43 (2005) 251-261.
[76] A.S.Y. Lee, P.J. Kranzusch, J.A. Doudna, J.H.D. Cate, eIF3d is an mRNA cap-binding protein that is required for specialized translation initiation, Nature, 536 (2016) 96-100.
[77] P. Crozet, L. Margalha, A. Confraria, A. Rodrigues, C. Martinho, M. Adamo, C.A. Elias, E. Baena-González, Mechanisms of regulation of SNF1/AMPK/SnRK1 protein kinases, Frontiers in Plant Science, 5 (2014) Article 190.
[78] C.M. Figueroa, J.E. Lunn, A tale of two sugars: trehalose 6-phosphate and sucrose, Plant Physiology, 172 (2016) 7-27.
[79] B. Wurzinger, A. Mair, K. Fischer-Schrader, E. Nukarinen, V. Roustan, W. Weckwerth, M. Teige, Redox state-dependent modulation of plant SnRK1 kinase activity differs from AMPK regulation in animals, FEBS letters, 591 (2017) 3625-3636.
[80] E. Lewandowska-Gnatowska, L. Szymona, M. Łebska, J. Szczegielniak, G. Muszyńska, Phosphorylation of maize eukaryotic translation initiation factor on Ser2 by catalytic subunit CK2, Molecular and Cellular Biochemistry, 356 (2011) 241-251.
[81] J.J. Mulekar, E. Huq, Expanding roles of protein kinase CK2 in regulating plant growth and development, Journal of Experimental Botany, 65 (2013) 2883-2893.
[82] I.C. Vélez-Bermúdez, M. Riera, Maize RNA-Binding Protein ZmTGH: A New Partner for CK2β1 Regulatory Subunit, in: K. Ahmed, O.-G. Issinger, R. Szyszka (Eds.) Protein Kinase CK2 Cellular Function in Normal and Disease States, Springer International Publishing, Cham, 2015, pp. 49-55.
[83] J. Zhu, W.-S. Wang, D. Ma, L.-Y. Zhang, F. Ren, T.-T. Yuan, A role for CK2 β subunit 4 in the regulation of plant growth, cadmium accumulation and H_2O_2 content under cadmium stress in *Arabidopsis thaliana*, Plant Physiology and Biochemistry, 109 (2016) 240-247.
[84] J. Chen, Y. Wang, F. Wang, J. Yang, M. Gao, C. Li, Y. Liu, Y. Liu, N. Yamaji, J.F. Ma, J. Paz-Ares, L. Nussaume, S. Zhang, K. Yi, Z. Wu, P. Wu, The rice CK2 kinase regulates trafficking of phosphate transporters in response to phosphate levels, The Plant Cell, 27 (2015) 711-723.
[85] M.K. Tarrant, H.-S. Rho, Z. Xie, Y.L. Jiang, C. Gross, J.C. Culhane, G. Yan, J. Qian, Y. Ichikawa, T. Matsuoka, N. Zachara, F.A. Etzkorn, G.W. Hart, J.S. Jeong, S. Blackshaw, H. Zhu, P.A. Cole, Regulation of CK2 by phosphorylation and O-GlcNAcylation revealed by semisynthesis, Nature Chemical Biology, 8 (2012) 262-265.

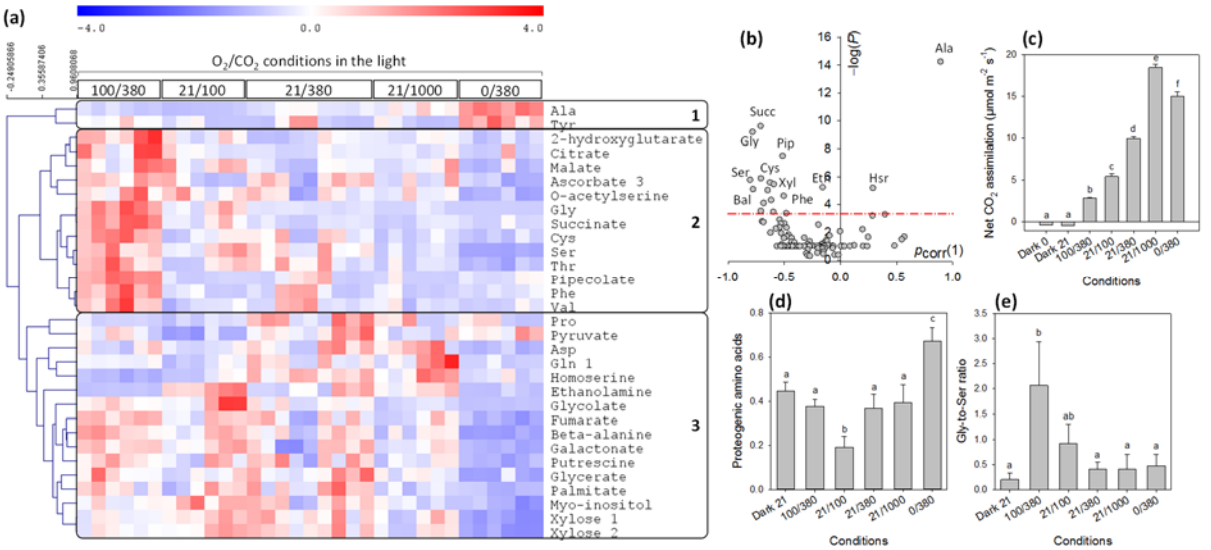

Fig. 1. Metabolism of Arabidopsis rosettes under different O_2/CO_2 conditions. (a) Heat map showing metabolites (from GC-MS metabolomics profiling) significantly different between O_2/CO_2 conditions in the light using a one-way ANOVA ($P<0.01$). Hierarchical clustering (Pearson correlation) is shown on left. Metabolite contents (mean-centered values) are shown with colors (color scale on top). Since most metabolites change considerably in darkness, dark conditions are not included in the heat map so as to show metabolites only significantly affected by photosynthetic conditions per se. Main groups identified by clustering are boxed and labelled with numbers. For each O_2/CO_2 condition, the $n = 6$ samples are shown, except under standard conditions (21% O_2-380 µmol mol^{-1} CO_2) where $n = 9$. (b) Volcano plot showing most discriminating metabolites, with –log(*P*-value) (*y* axis) and the loading in the OPLS analysis ($p_{corr}(1)$; *x* axis). The red dash-dotted line stands for the Bonferroni threshold. (c) Photosynthesis (net CO_2 assimilation) measured by gas exchange. (d) Total content in proteogenic amino acids (relative to internal standard, ribitol, and normalized to DW). (e) Glycine-to-serine ratio. In (a), numbers on right refer to groups (metabolite clusters) discussed in main text. Numbers associated with metabolite names refer to distinct derivatives (analytes) of the same metabolite. In (c-e), letters stand for statistical classes ($P<0.05$). In (c), the rate of CO_2 evolution (respiration) in darkness is also indicated (either in 0% or 21% O_2) and in (d-e), values obtained in the dark at 21% O_2 are also shown. **Abbreviations**: Bal, β-alanine; Cys, cysteine; Etn, ethanolamine; Gly, glycine; Hsr, homoserine; Phe, phenylalanine; Pip, pipecolate; Pro, proline; Ser, serine; Succ, succinate; Thr, threonine; Val, valine; Xyl, xylose. A magnified version of this figure is available as Fig. S7.

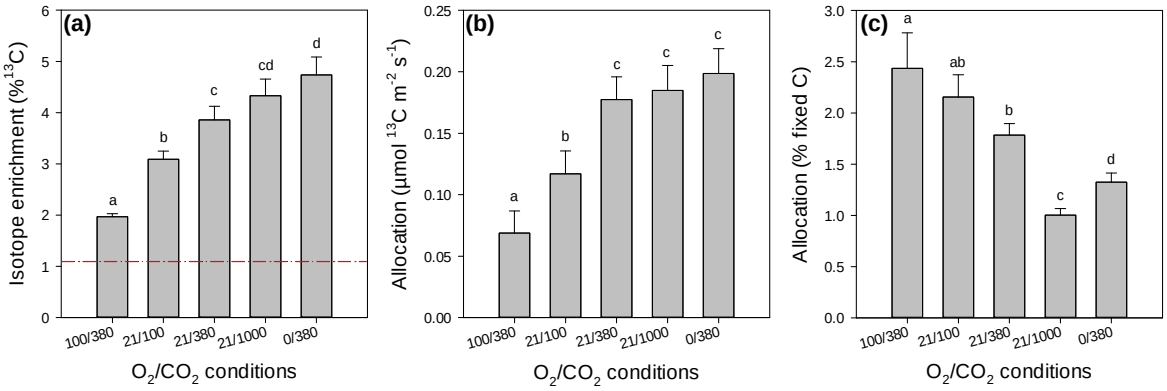

Fig. 2. Carbon allocation to protein synthesis determined by $^{13}CO_2$ labelling in the light. (a) Isotope enrichment (% ^{13}C) in proteins, measured by isotope ratio mass spectrometry (EA-IRMS) on purified proteins. (b) Allocation of ^{13}C to protein (apparent flux to protein synthesis). (c) Allocation expressed in percentage of photosynthesis (^{13}C partition to protein synthesis) calculated from (b) and photosynthesis (given in Fig. 1). In (a), the red dash-dotted line stands for ^{13}C natural abundance (enrichment in proteins measured after gas exchange carried out with ordinary CO_2). In (b-c), the contribution of natural abundance has been subtracted. Letters stand for statistical classes (P<0.05).

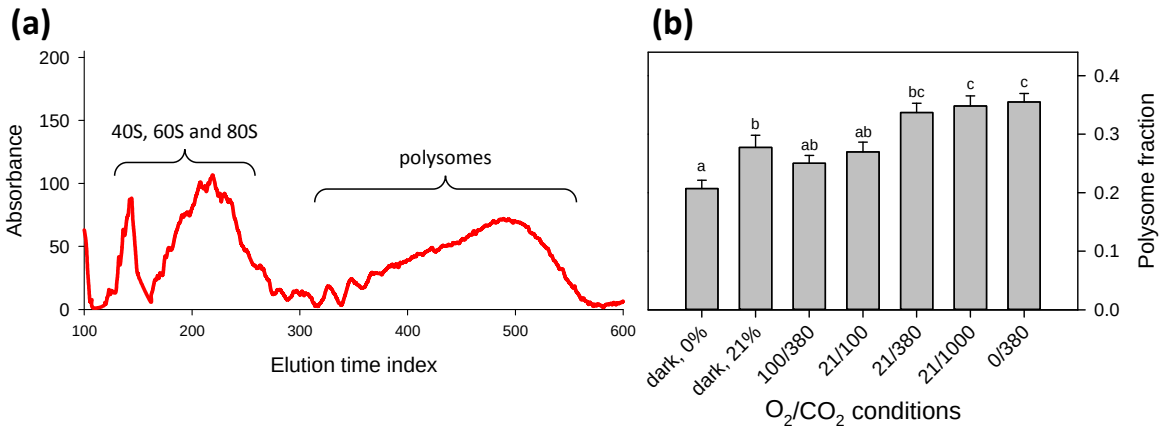

Fig. 3. Polysome abundance determined with gradient separation and absorbance at 260 nm. (a) Typical background-subtracted absorbance profile (standard conditions, 21% O2, 380 µmol mol^{-1} CO_2) showing the oscillating peak region on right corresponding to polysomes (legend after [68]). (b) Quantitation of polysome fraction from background-subtracted traces, in % of total signal. In (b), letters stand for statistical classes (P<0.05). Note that (b) also shows results obtained in darkness at either 0% or 21% O_2, with a significant down-regulating effect of anoxia on polysome abundance.

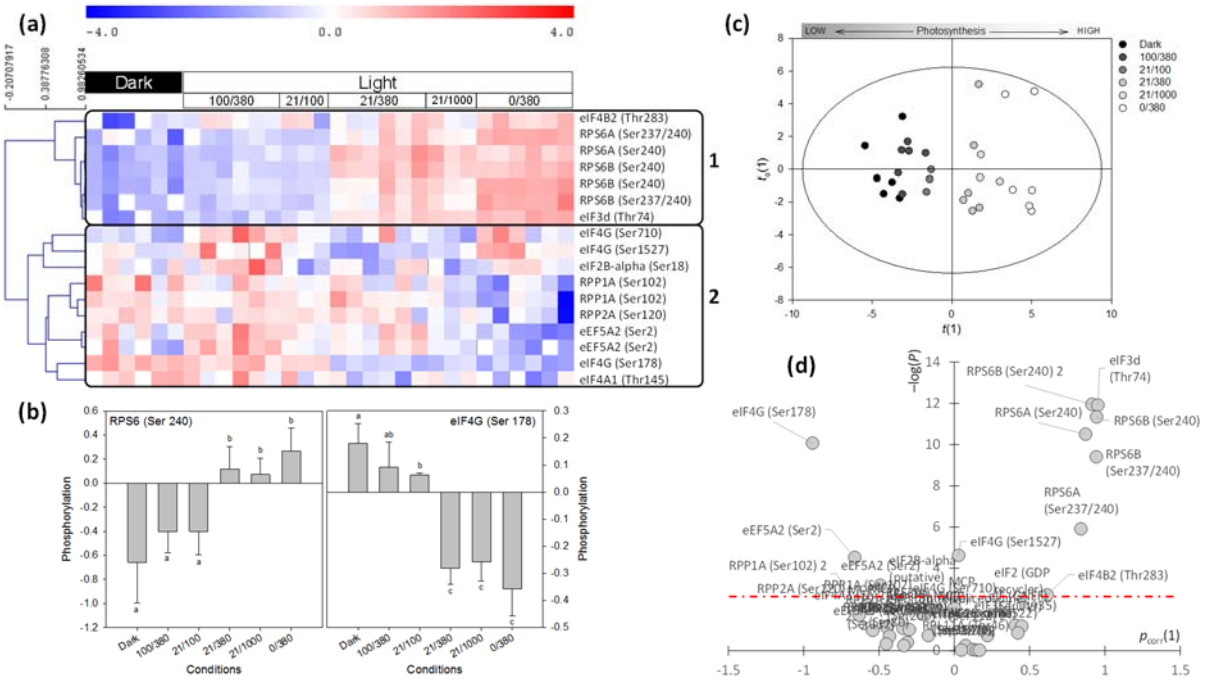

Fig. 4. Phosphorylation pattern of molecular actors involved in translation. (a) Heat map showing significant phosphosites with $P < 0.05$, with a hierarchical clustering on left (Pearson correlation). Main groups found by clustering are boxed and labelled 1 and 2. When phosphosite identifiers appear several times (e.g. RPS6A Ser240), it refers to analytically different phosphopeptides. "Dark" refers to darkness at 21% O_2. In the light, O_2/CO_2 conditions are recalled (%/ppm). (b) Lookup of average phosphorylation at Ser 204 in RPS6A and RPS6B (left) and Ser 178 in eIF4G (right). Letters stand for statistical classes ($P < 0.05$). (c) Score plot of the OPLS multivariate analysis using photosynthetic conditions as a quantitative variable (aligned along the *x* axis). (d) Volcano plot combining univariate (–log(*P*) from ANOVA) and multivariate (loading $p_{corr}(1)$ from the OPLS) analyses showing most significant phosphosites. Red dash-dotted line, Bonferroni threshold ($P = 0.0014$). A magnified version of this figure is available as Fig. S8.

Table 1. List of phosphopeptides found here, associated with protein synthesis. The column "New" indicates phosphosites that are absent from (Boex-Fontvieille et al. 2014) and references therein, and the database Phosphat 4.0 (http://phosphat.uni-hohenheim.de/). "Occ." Indicates when a phosphopeptide was found to be occasionally detected, that is, missing across more than 20% of the samples. Statistics reported in Fig. 4 only used non-occasional phosphopeptides, that is, with less than 20% missing values. In the column "Comments", the term "common to" means that the phosphopeptides (with the same sequence) can also be found in other isoforms of the protein, but disambiguation could be done here. The nomenclature for eEFs and eIFs is after [12], except for the ubiquitin-binding elongation factor eEF1B (AT5G53330) which is recognized as an elongation factor in TAIR but is not listed in [12] and is also refered to as a cell wall proline-rich protein in Protein Data Bank.

ATG number	Name	Phosphosite	Comments	New	Sequence	Occ.
Elongation factors (eEF)						
AT1G07920	eEF1-alpha	Thr82			FE**(pT)**TKYYCTVIDAPGHR	Yes
AT1G30230	eEF1B-beta	Thr91			ISGVSAEGSGVIVEGSAPITEEAVA**(pT)**PPAADSK	Yes
AT5G53330	eEF1B-related	Ser58	Ubiquitin-binding elongation factor		N**(pS)**SFQHNTSPSSGIGIR	Yes
AT1G69410	eEF5A3	Ser2			**(pS)**DDEHHFESSDAGASK	
AT1G26630	eEF5A2	Ser2			M**(pS)**DDEHHFEASESGASK	
		Ser2			**(pS)**DDEHHFEASESGASK	
Initiation factors (eIF)						
AT2G34970	eIF2B-epsilon	Thr522			DKLSEITQAIDDDD**(pT)**DDESVVPTSGELK	
AT1G48970	eIF2B-delta 2	Ser149		Yes	LSA**(pS)**LPNGGFDLTLAVR	
AT1G72340	eIF2B-alpha	Ser18			RSSN**(pS)**PPMADTTR	
		Ser18			SSN**(pS)**PPMADTTR	Yes
AT5G38640	eIF2B-delta 1	Ser126			SSVPVA**(pS)**SLPGIGMDSMAAAK	Yes
		Ser88			VAVAGAAASAV**(pS)**PSSFSYSSR	Yes
		Thr230			A**(pT)**SQKNDVAVATGAAEK	Yes
		Ser108			DFPDGSTTA**(pS)**PGR	Yes
		Ser108			RDFPDGSTTA**(pS)**PGR	
		Ser69			LN**(pS)**SDTFPLR	Yes
AT5G25780	eIF3B2	Ser684	common to eIF3B1		QNLRDGEV**(pS)**DVEEDEYEAK	Yes
AT3G56150	eIF3C1	Tyr35			**(pY)**LQSGSEDDDDTDTKR	
		Ser38/40			YLQ(s)G(s)EDDDDTDTKR	
AT4G20980	eIF3d	Thr74			NLSNPSARPN**(pT)**GSK	
AT3G13920	eIF4A1	Ser4			AG**(pS)**APEGTQFDAR	Yes
		Thr145	common to eIF4A2		VHACVGG**(pT)**SVR	
AT3G26400	eIF4B1	Ser237			**(pS)**STFGSSFGDSGQEER	Yes
AT1G13020	eIF4B2	Thr283			KADTEVSE**(pT)**PTAVK	
AT3G60240	eIF4G	Ser178			TT**(pS)**APPNMDDQKR	
		Ser710			STEGSSHASSEISGS**(pS)**PQEK	
		Ser1527			QVLQGPSATVN**(pS)**PR	
AT2G24050	eIFiso4G2	Ser512		Yes	**(pS)**LSVNSR	Yes
AT1G77840	eIF5	Ser200			NH**(pS)**SDEDISPK	
		Ser200/201			NH(s)(s)DEDISPK	Yes

Other molecular actors						
AT1G64790	ILA	Ser1887	ILITHYIA (activator of GCN2 and thus of eIF2)		ALLEGG**(pS)**DDEGASTEAQGR	Yes
AT1G80930	MCP	Ser187	MIF4G domain-containing spliceosome subunit		VIADKP**(pS)**DEEDDR	
		Ser187			VIADKP**(pS)**DEEDDRQR	
		Ser80			RKET**(pS)**DDEELAR	
		Ser112			IEVD**(pS)**DGDGERR	
		Ser112			RIEVD**(pS)**DGDGER	
AT1G48920	NUC-L1	Ser163	Nuclear RNA binding protein L1 (ribosome synthesis)		ESSSEDDS**(pS)**SEDEPAKKPAAK	Yes
Ribosomal proteins						
AT3G58660	RPL10E	Ser6			TTAV**(pS)**PPPPQEQQLVHASQTSR	Yes
AT2G42740	RPL11A	Thr46	common to RPL11B, RPL11C and RPL11D		VLEQLSGQ**(pT)**PVFSK	
AT5G23900	RPL13D	Thr138			AGDS**(pT)**PEELANATQVQGDYMPIASVK	Yes
AT3G09200	RPP0B	Ser305			VEEKEE**(pS)**DEEDYGGDFGLFDEE	Yes
AT3G11250	RPP0C	Ser308			KEE**(pS)**DEEDYEGGFGLFDEE	Yes
		Ser308			VEEKKEE**(pS)**DEEDYEGGFGLFDEE	Yes
AT1G01100	RPP1A	Ser102	common to RPP1B and RPP1C		KDEPAEE**(pS)**DGDLGFGLFD	
		Ser102	common to RPP1B and RPP1C		KKDEPAEE**(pS)**DGDLGFGLFD	
AT2G27720	RPP2A	Ser120	common to RPP2B and RPP2D		EEKKEEKEE**(pS)**DDDMGFSLFE	Yes
		Ser120	common to RPP2B and RPP2D		KEEKEE**(pS)**DDDMGFSLFE	
AT2G27710	RPP2B	Ser120	common to RPP2A and RPP2D		EEKKEEKEE**(pS)**DDDMGFSLFE	Yes
		Ser120	common to RPP2A and RPP2D		KEEKEE**(pS)**DDDMGFSLFE	
		Ser77			LASVPSGGGGGVAVA**(pS)**ATSGGGGGGGASAAESK	Yes
AT5G57290	RPP3B	Ser90	common to RPP3A		KEE**(pS)**EEEEGDFGFDLFG	Yes
		Ser90	common to RPP3A		KKEE**(pS)**EEEEGDFGFDLFG	Yes
AT2G45710	RPS27A	Ser29	common to RPS27B and RPS27C		LVQ**(pS)**PNSFFMDVK	
AT2G41840	RPS2C	Ser273			AL**(pS)**TSKPDPVVEDQA	Yes
AT3G04840	RPS3Aa	Ser236			LMDVHGDY**(pS)**AEDVGVK	
AT4G31700	RPS6A	Ser240			L**(pS)**SAAAKPSVTA	Yes
		Ser240			SRL**(pS)**SAAAKPSVTA	
		Ser237/240			(s)RL(s)SAAAKPSVTA	
AT5G10360	RPS6B	Ser240			L**(pS)**SAPAKPVAA	
		Ser240			SRL**(pS)**SAPAKPVAA	
		Ser237/240			(s)RL(s)SAPAKPVAA	
AT1G74970	RPS9 (chloroplastic)	Ser47/Thr51		Yes	RA(s)LSITA(t)VSAPPEEEEIVELKK	Yes
AT5G15200	RPS9B	Ser68			DLLTLDEK**(pS)**PR	Yes